CCFE-PR(15)64

H. Zhu, R.O. Dendy, S.C. Chapman, and S. Inagaki

A quantitative model for heat pulse propagation across Large Helical Device plasmas

A quantitative model for heat pulse propagation across Large Helical Device plasmas

H. Zhu,[1] R.O. Dendy,[2, 1, 3, 4] S.C. Chapman,[1, 5, 6] and Inagaki[3, 4]

[1]Centre for Fusion, Space and Astrophysics, Department of Physics, Warwick University, Coventry CV4 7AL, United Kingdom

[2]CCFE, Culham Science Centre, Abingdon, Oxfordshire OX14 3DB, United Kingdom
[3]Itoh Research Center for Plasma Turbulence, Kyushu University, Kasuga 816-8580, Japan
[4]Research Institute for Applied Mechanics, Kyushu University, Kasuga 816-8580, Japan
[5]Max Planck Institute for the Physics of Complex Systems, Dresden, Germany
[6]Department of Mathematics and Statistics, University of Tromsø, Tromsø, Norway

A quantitative model for heat pulse propagation across Large Helical Device plasmas

H. Zhu,[1] R.O. Dendy,[2,1,3,4] S.C. Chapman,[1,5,6] and S. Inagaki[3,4]

[1]*Centre for Fusion, Space and Astrophysics, Department of Physics, Warwick University, Coventry CV4 7AL, United Kingdom*

[2]*CCFE, Culham Science Centre, Abingdon, Oxfordshire OX14 3DB, United Kingdom*

[3]*Itoh Research Center for Plasma Turbulence, Kyushu University, Kasuga 816-8580, Japan*

[4]*Research Institute for Applied Mechanics, Kyushu University, Kasuga 816-8580, Japan*

[5]*Max Planck Institute for the Physics of Complex Systems, Dresden, Germany*

[6]*Department of Mathematics and Statistics, University of Tromsø, Tromsø, Norway*

Abstract

It is known that rapid edge cooling of magnetically confined plasmas can trigger heat pulses that propagate rapidly inward. These can result in large excursion, either positive or negative, in the electron temperature at the core. A set of particularly detailed measurements was obtained in Large Helical Device(LHD) plasmas [S. Inagaki *et al, Plasma Phys. Control. Fusion* **52** (2010) 075002], which are considered here. By applying a travelling wave transformation, we extend the model of R. O. Dendy, S. C. Chapman and S. Inagaki, *Plasma Phys. Control. Fusion* **55** (2013) 115009, which successfully describes the local time-evolution of heat pulses in these plasmas, to include also spatial dependence. The new extended model comprises two coupled nonlinear first order differential equations for the (x, t) evolution of the deviation from steady state of two independent variables: the excess electron temperature gradient and the excess heat flux, both of which are measured in the LHD experiments. The mathematical structure of the model equations implies a formula for the pulse velocity, defined in terms of plasma quantities, which aligns with empirical expectations and is within a factor of two of the measured values. We thus model spatio-temporal pulse evolution, from first principles, in a way which yields as output the spatiotemporal evolution of the electron temperature, which is also measured in detail in the experiments. We compare the model results against LHD datasets using appropriate initial and boundary conditions. Sensitivity of this nonlinear model with respect to plasma parameters, initial conditions and boundary conditions is also investigated. We conclude that this model is able to match experimental data for the spatio-temporal evolution of the temperature profiles of these pulses, and their propagation velocities, across a broad radial range from $r/a \simeq 0.5$ to the plasma core. The model further implies that the heat pulse may be related mathematically to soliton solutions of the Korteweg-de Vries-Burgers equation.

Keywords: wave propagation, travelling wave transformations, nonlinear phenomena, Large Helical Device

1. Introduction

The transport of energy across magnetically confined fusion plasmas, and the storage of energy within them, reflects a wide range of turbulent and nonlinear phenomenology; see for example, Refs.[1–32]. There is extensive experimental evidence for transport phenomena that are non-diffusive and may be non-local. Examples have been found in many tokamak plasmas, for example JET[12, 13], DIII-D[14–16], JT-60U[17], HL-2A[18], Alcator C-Mod[19], TEXTOR[20], TEXT[21], RTP[22] and TFTR[23], as well as in the LHD stellarator-torsatron[17, 24–27]. A broad range of techniques for data analysis, see for example Refs.[12, 14, 28], have been used to identify various forms of perturbation of heat and particle fluxes from their steady states, see the reviews[29, 30]. Measurements of the spatio-temporal propagation of strongly nonlinear localised heat pulses provide a particularly interesting, and potentially fruitful, challenge to theoretical understanding and models. Here we focus on cold pulse experiments, see for example Ref.[18, 19, 24]. These cold pulses are typically initiated by injection into the edge plasma of ice pellets or supersonic molecule beams, by gas puffing, and by laser ablation. The zero-dimensional model of Ref.[25], which incorporates only time dependence, is successful in quantitatively capturing the local time evolution of $\delta\nabla T_e$ and $\delta\boldsymbol{q_e}$ at a specific radius during two well diagnosed cold heat pulse experiments[24] using pellet injection in LHD; we refer in particular to Figs.3 and 5 of Ref.[25]. This motivates the following physical conjecture, which we test in the present paper. The zero-dimensional model is known to work at the best diagnosed spatial location, capturing the time evolution of the pulse there, where $t = 0$ is defined to be the local arrival time of the initial impulsive perturbation. Therefore we conjecture that the zero-dimensional model ought to work at each location across the radial domain of the plasma within which the same physical processes determine the behaviour of the pulse. From this we infer that the model ought to apply in a frame that is co-moving radially with the heat pulse across this region. This final step in the conjecture provides a simple path to construct a spatio-temporally dependent model from the tested time-dependent-only model of Ref.[25]. We apply a travelling wave transformation by replacing t in Eqs.(1-3) of Ref.[25] by $\xi = x + v_0 t$; here v_0 is to be considered as a proxy of the pulse propagation velocity in the radial direction x, and the sign convention adopted for t assists consideration of inward propagation. Importantly, as we shall show, the mathematical structure of the resultant model equations,

combined with the choice of physical model parameters that carries over from Ref.[25], yield a formula for v_0 that aligns with prior empirical expectations.

2. Model description

The normalised zero-dimensional model[25] examined below is constructed in terms of the three key physical quantities that were measured[24] so as to characterise pulse propagation in LHD. These quantities are the deviation from steady state of the electron temperature gradient $\delta\nabla T_e$, the excess turbulent heat flux $\delta\boldsymbol{q_e}$, and the deviation δT_e of electron temperature from its steady-state value. The dimensionless counterparts of these variables are denoted by x_1, x_2 and x_3 respectively, as defined in Ref.[25]. The model of Ref.[25] shows quantitative agreement between its outputs and experimental measurements of the time evolution of these variables at fixed locations in the LHD plasma, after rapid cooling at the edge. It is successful both when core electron temperature rises on arrival of the pulse, and when it drops. However, for given parameters and initial conditions, the model only simulates the time evolution of a passing heat pulse at a specific radius, for example $r/a = 0.19$ in [25]. Spatial dependence is eliminated from the physical picture underlying the model in Ref.[25] by using the parameter $1/L_c$ as a proxy for divergence in the heat flux energy conservation equation; here L_c is the characteristic scale-length of steady-state turbulent transport. The model equations (5) to (7) of Ref.[25] are as follows

$$\frac{dx_1}{dt} = \kappa_{T0}x_2 + x_1x_2\frac{\partial\kappa_T}{\partial x_1} + x_2x_3\frac{\partial\kappa_T}{\partial x_3} - \gamma_{L1}x_1 \tag{1}$$

$$\frac{dx_2}{dt} = -\kappa_{Q0}x_1 - x_1^2\frac{\partial\kappa_Q}{\partial x_1} - x_1x_3\frac{\partial\kappa_Q}{\partial x_3} - \gamma_{L1}x_2 \tag{2}$$

$$\frac{dx_3}{dt} = -\frac{1}{\tau_c}\frac{\eta}{\chi_0}x_2 - \gamma_{L2}x_3 \tag{3}$$

Physically, Eqs.(1) to (3) embody on assumption of dominant strong coupling between $\delta\nabla T_e$ and $\delta\boldsymbol{q_e}$, while the background transport acts to dissipate the pulse. The physical significance of the various coefficients is described in the discussion of equations (1) to (4) of Ref.[25]. We note that, from Eq.(3) above, x_3 is slave to x_2 because the electron temperature deviation from steady state is damped linearly and by excess turbulent transport which scales with x_2. Thus x_3 is not an independent variable in the model, although plotting x_3 is valuable for model validation.

Central to the present paper is the adoption of travelling wave transformations as a method for generating (x,t)–dependence from the t–dependent model of Eqs.(1) to (3). We assume that

$$x_i\left(x,t\right)=y_i\left(\xi\right),\xi=x+v_0t \qquad i=1,2,3 \tag{4}$$

Here x and t are considered to be independent variables, and we refer to v_0 as the pseudo-velocity of the pulse. This pseudo-velocity is expected to be similar, but not identical, to the real measured velocity of the pulse. It then follows that

$$\frac{dx_i}{dt}=\frac{dy_i}{d\xi}\frac{\partial\xi}{\partial t}=v_0\frac{dy_i}{d\xi} \qquad i=1,2,3 \tag{5}$$

Due to the fact that y_3 is a dependent variable, we choose to simplify by neglecting all y_3 related terms in Eqs.(1) to (3), and substitute Eq.(5) into Eqs.(1-2), yielding

$$-v_0\frac{dy_1}{d\xi}=\kappa_{T0}y_2+y_1y_2\frac{\partial\kappa_T}{\partial y_1}-\gamma_{L1}y_1 \tag{6}$$

$$-v_0\frac{dy_2}{d\xi}=-\kappa_{Q0}y_1-y_1^2\frac{\partial\kappa_Q}{\partial y_1}-\gamma_{L1}y_2 \tag{7}$$

Our new model Eqs.(6-7) comprises only two independent variables: y_3 values are deduced directly from the timeseries of y_2, using Eq.(3) above. Let us now operate on Eq.(6) with $d/d\xi$ and multiply Eq.(7) by κ_{T0}, then eliminate $dy_2/d\xi$ by substitutions. This yields the following equation after leading order approximation and transpositions:

$$v_0\frac{d^2y_1}{d\xi^2}-\gamma_{L1}\frac{dy_1}{d\xi}+\left(\frac{\kappa_{T0}}{v_0}\frac{\partial\kappa_Q}{\partial y_1}+\frac{\kappa_{Q0}}{v_0}\frac{\partial\kappa_T}{\partial y_1}\right)y_1^2+\frac{\kappa_{T0}\kappa_{Q0}}{v_0}y_1=-\frac{\kappa_{T0}\gamma_{L1}}{v_0}y_2+\frac{\kappa_{T0}}{v_0}\frac{\partial\kappa_T}{\partial y_1}y_2^2 \tag{8}$$

The second coupled nonlinear ordinary differential equation is derived by applying similar procedures:

$$v_0\frac{d^2y_2}{d\xi^2}-\gamma_{L1}\frac{d^2y_2}{d\xi^2}+\frac{\kappa_{T0}\kappa_{Q0}}{v_0}y_2=\frac{\kappa_{Q0}\gamma_{L1}}{v_0}y_1-y_1y_2\left(\frac{\kappa_{Q0}}{v_0}\frac{\partial\kappa_T}{\partial y_1}+2\frac{\kappa_{T0}}{v_0}\frac{\partial\kappa_Q}{\partial y_1}\right) \tag{9}$$

Equations (8) and (9) comprise our mathematical model for the propagating heat pulse. Its physical motivation is that of Ref.[25], combined with the co-moving conjecture outlined above and expressed in Eq.(4). The mathematical structure of Eq.(8) can be linked, in certain approximations, to the Korteweg-de Vries-Burgers(KdV-Burgers) equation[31], and Eq.(9) can be linked to a damped wave equation in the co-moving frame. In particular, the left hand side of Eq.(8) corresponds to that in the formulation of the KdV-Burgers equation in Eq.(5.3) of Ref.[31]. This is known to support soliton pulses that move at a speed determined by the coefficient of the term which multiplies y_1. This motivates the following conjecture regarding heat pulse velocity in our model:

$$v_0 \sim \left(\kappa_T \kappa_Q\right)^{1/2} \tag{10}$$

This scaling has previously been noted empirically from heat pulse experiments[29, 32]. From those references, we can also infer that $v_0 \sim \left(\chi_0 \left(\kappa_T \kappa_Q\right)^{1/2}\right)^{1/2}$ or $v_0 \sim \left(\eta \left(\kappa_T \kappa_Q\right)^{1/2}\right)^{1/2}$. The empirical value of the pulse speed, which may be expected to align with the empirical value of the pseudo-velocity defined by Eq.(10), is obtained from the LHD datasets below.

3. Comparison of model results with LHD experimental data

We recall that y_1, y_2 and y_3 are the dimensionless counterparts of $\delta\nabla T_e, \delta\boldsymbol{q_e}$ and δT_e respectively. Solution of our model, embodied in the two coupled nonlinear ordinary differential equations Eqs.(8) and (9), proceeds as follows. The numerical values for κ_T, κ_Q and their derivatives, together with the numerical values of $\gamma_{L1}, \gamma_{L2}, \eta, \tau_c$ and χ_0, carry over identically from Ref.[25], to which we refer for the experimental motivation for these values; see Table I for detailed information.

Parameter / Case	κ_{T0}	$\partial\kappa_T/\partial x_1 = \partial\kappa_T/\partial x_3$	κ_{Q0}	$\partial\kappa_Q/\partial x_1 = \partial\kappa_Q/\partial x_3$	$\gamma_{L1} = \gamma_{L2}$	χ_0	$\eta = 2\chi_0/3$	$\eta/\tau_c\chi_0$
T_e Rise(R)	15	1.5	225	22.5	35	3.2	2.13	10.5
T_e Drop(D)	20	2.0	400	40.0	35	3.2	2.13	10.5

Table I. Experimentally inferred parameter values[25] for both T_e rise and T_e drop cases.

The new model embodied in Eqs.(8) and (9) is strongly nonlinear. In solving it, we have three kinds of degrees of freedom. First, there are the initial values of $y_i^{'}(\xi = 0)$. Second, there is the value of the pseudo-velocity v_0. Third, it is possible to apply fixed horizontal and vertical shifts in the values of the electron temperature and time, provided these shifts are applied uniformly to all outputs of a simulation, as a way of reducing systematic errors introduced by parameter choices. We optimise model outputs, for comparison with the experimental measurements, in these three ways. These model outputs (time traces of y_1, y_2 and y_3) reflect the underlying phase space structure of the solutions of the nonlinear system of equations. This structure is robust, in the sense discussed in Ref.[25], and as demonstrated for the present system of equation in Fig.7 below, for example. We recall also that the great majority of model parameter values, see e.g. Table I, are determined by experimental measurements.

The boundary conditions on the $y_i,\ i = 1, 2, 3$ and their derivatives, evaluated at $\xi = 0$ and $\xi = 10$ which define the solution domain, coincide with the experimentally motivated values in Ref.[25] where these carry over. Specifically $y_1(\xi = 0) = y_1(\xi = 10) = 0$; $y_2(\xi = 0) = -1.5, y_2(\xi = 10) = 0$ and $y_3(\xi = 0) = 0.01$ for the core electron temperature Rise(R) case in LHD plasma 49708. We take $y_1(\xi = 0) = y_1(\xi = 10) = 0$; $y_2(\xi = 0) = 1, y_2(\xi = 10) = 0$ and $y_3(\xi = 0) = -0.01$ for the core electron temperature Drop(D) case in LHD plasma 49719. Boundary conditions unspecified in Ref.[25], which are needed in order to satisfy the boundary conditions above, are assumed to be as follows here: $y_1'(\xi = 0) = -1.496$ and $y_2'(\xi = 0) = 3.552$ for R case; $y_1'(\xi = 0) = 0.668$ and $y_2'(\xi = 0) = -1.156$ for D case. Table II lists all boundary conditions.

Boundary Condition / Case	$y_1(\xi = 0) = y_1(\xi = 10)$	$y_2(\xi = 0)$	$y_2(\xi = 10)$	$y_3(\xi = 0)$	$y_1^{'}(\xi = 0)$	$y_2^{'}(\xi = 0)$
T_e Rise(R)	0	-1.5	0	0.01	-1.496	3.552
T_e Drop(D)	0	1.0	0	-0.01	0.668	-1.156

Table II. Boundary conditions of both T_e rise and T_e drop cases.

Figure 1 compares time traces of the evolving electron temperature at multiple radial

locations, obtained from the model and from experimental data(# Te49708) for the R case. Several representative radii are marked by arrows on the right hand side. The model results are able to match experimental data from $\rho = 0.45$ inward to the core, if we uniformly apply horizontal(+0.01) and vertical(+0.20) shifts, suggesting that the model applies over this broad radial range. It is also clear that electron temperature profiles from $\rho = 0.546$ outward to $\rho = 0.703$ are not simulated by the model. This suggests that different physics dominates heat pulse propagation in the outer region of this plasma. Figure 2 demonstrates the comparison of model results and experimental data(# Te49719) for the D case. In common with the R case shown Fig.1, the model results are good from $\rho = 0.450$ inward to the core, with uniformly applied horizontal(+0.04) and vertical(+0.07) shifts, but not in the outer region of this plasma. Fig.3 and Fig.4 show zoomed-in electron temperature pulse plots at three specific radii, selected from Fig.1 and Fig.2 respectively.

Empirically, we approach v_0 by identifying a best fit straight line linking the positions of the peak or trough of the heat pulse temperature profile in the two cases, see Figs.5 and 6. The effect of data noise on peak location is minimised by taking a five per cent running window. The width of the filter window determines the horizontal error bars. We assume, for simplicity and to match our travelling-wave model, that the inward radial propagation velocity of the heat pulse is invariant across the plasma volume of interest. A straight line fit to the radial location of the pulse peak versus time is thus applied. The error of this fitting may come from the radial dependence of the pulse velocity, which tends to increase in the central region. We find from Figs.5 and 6 that $v_0 = 15$ for the temperature rise case and $v_0 = 30$ for the temperature drop case. These dimensionless pseudo-velocity values equate to the dimensional values $(32.62 \pm 9.89) ms^{-1}$ and $(53.50 \pm 20.97) ms^{-1}$ respectively, which are comparable in magnitude to measured heat pulse propagation velocities. The ratio 2 between these two velocities is broadly consistent with the value inferred by substituting experimentally measured values for transport coefficients into Eq.(10). We have $v_0^D/v_0^R \sim \left(\kappa_T^D \kappa_Q^D / \kappa_T^R \kappa_Q^R\right)^{1/2} = 1.54 \simeq 2$, referring also to Table I, where superscripts R and D denote the core T_e rise and drop cases respectively. We note that the empirically determined velocities v_0^R and v_0^D of heat pulse propagation need not necessarily coincide with the optimal value of the mathematical transformation parameter v_0 in Eq.(4).

Mathematically, we may treat v_0 as a free parameter in Eqs.(8) and (9), which we have

labelled the pseudo-velocity. We solve Eqs.(8) and (9) repeatedly for different values of this pseudo-velocity, see for example Fig.7 for the R case, and identify the best fit value. To test sensitivity with respect to ξ, three other cases($\xi = 5; \xi = 15; \xi = 20$) have been examined. All three of these test options exhibit the same properties as the case of $\xi = 10$. Various combinations of initial conditions and pseudo-velocities were also tested, showing that the combination specified above provides the best fit to the experimental data. For the phase plots, see for example the right-hand panel of Fig.7, circulation directions are identical with those of the experimental data for both the R and D cases.

The fitting operation can be assisted by shifting the origin of co-ordinates. The robustness, with respect to variation of initial conditions, of this mathematical approach to identifying pseudo-velocity has been tested. This robustness reflects the structure of the underlying attractor in phase space, projected in (y_1, y_2) coordinates in these two figures; compare also Figs.6 and 7 of Ref.[25].

4. Conclusions

We have derived from first principles a time-dependent model in one spatial dimension, which is able to describe quantitatively the radial inward propagation of heat pulses in the core of two plasmas[24] in the Large Helical Device(LHD). In one plasma the central electron temperature rises, in the other it falls. This new model is derived from a travelling wave transformation of the zero-dimensional model of Ref.[25], which is known to capture the time-evolution of the heat pulse as it passes through a fixed radial location in these two plasmas. From the experimental data, we infer that the velocity of the propagating pulse is constant in both the electron temperature rise and drop cases. The pulse velocity in the electron temperature rise case is smaller than in the drop case by a factor $\simeq 2$. This aligns with Eq.(10), which reaches back into the mathematical structure of our model, and also coincides with empirical expectations given the values of the heat conduction parameters for these two plasmas. A pseudo-velocity parameter is introduced in the travelling wave transformations, in order to model heat pulse propagation across spatial location as well as in time. From numerical tests, we discover that real pulse velocity is about two times the best estimate of the travelling-wave transformation parameter v_0, referred to as the pseudo-velocity. Comparison between model outputs and raw experimental data suggests that our model is able to describe heat pulse propagation well, within a broad radial range of the

LHD core plasma from $r/a \simeq 0.5$ to the centre.

The results of the present paper provide additional support to the physical proposals, described in Sec.2 of Ref.[25], which motivate the simple model equations reproduced as Eqs.(1) to (3) above. Central to these proposals is the conjecture that heat pulses are structures which are so strongly nonlinear that their evolution is primarily determined by the reactions of the perturbed heat flux and the perturbed temperature gradient on each other, while turbulent transport plays a relatively minor dissipative role. It is this mutually coupled interaction that governs the local plasma dynamics of the heat pulse in space, equivalent to the local up-and-down dynamics of a water wave under gravity. We have shown in this paper that this coupling model lends itself readily to a travelling wave transformation, yielding spatio-temporal pulse propagation, and that the pulse velocity that emerges mathematically provides an adequate match to empirical results and expectations. This aspect of the analysis also provides guidance on a previously unanswered question, namely the generic character of the heat pulse: we have shown that it may be closely related to a Korteweg-de Vries-Burgers soliton. Two avenues of investigation would repay immediate attention. First, this model has been tested on, and motivated by, measurements from only two plasmas in LHD - albeit plasmas with exceptionally high quality measurements. The simplicity of the model encourages one to hope that it may be more widely applicable, and clearly it should now be tested on a broader range of heat pulse experimental datasets, provided that they possess the required spatial and temporal resolution and that the other relevant plasma parameters are well diagnosed, as in LHD. Second, while gyrokinetic or other computationally intensive transport simulations have not yet (to the authors' knowledge) been applied to heat pulse experiments, the outputs of any future simulations of heat pulses could be tested directly against the analytical model presented here, which is constructed in terms of variables that are directly measurable, as distinct from the first-principles particle and field distributions of gyrokinetic theory.

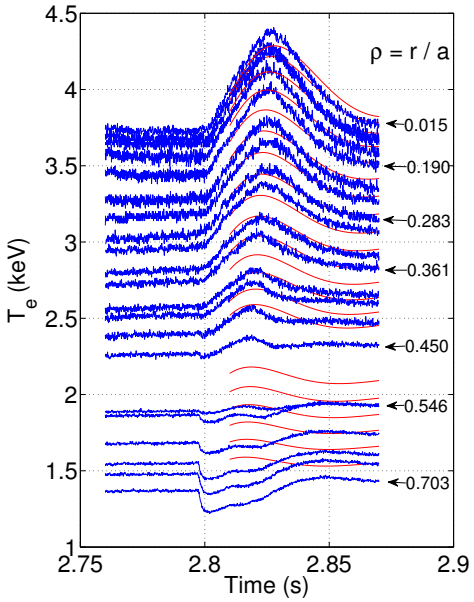

Figure 1. Time evolution of electron temperature at multiple radial locations, derived from LHD data(blue) and the model(red) for the core temperature rise(R) heat pulse propagation experiment in plasma 49708. Radial locations range from edge($\rho = 0.703$) to core($\rho = 0.015$), where $\rho = r/a$, r is the radial co-ordinate and $a \sim 0.6$m is minor radius of LHD. Model results match experimental data well from $\rho = 0.450$ inwards to the plasma core, especially amplitudes and the time structure of pulse decay. The amplitudes of model time traces increase from edge to core, as in the measured electron temperature profiles. Model results do not fit experimental data outwards from $\rho = 0.546$ to $\rho = 0.703$, implying that different physics applies in the outer LHD plasma.

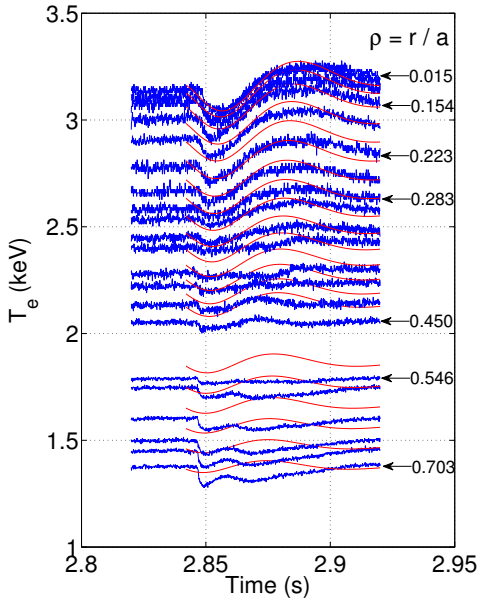

Figure 2. Time evolution of electron temperature at multiple radial locations, derived from LHD data(blue) and the model(red) for the core temperature drop(D) heat pulse propagation experiment in plasma 49719. Radial locations range from edge($\rho = 0.703$) to core($\rho = 0.015$), where $\rho = r/a$, r is the radial co-ordinate and $a \sim 0.6$m is minor radius of LHD. As in Fig.1, model results match experimental data well from $\rho = 0.450$ inwards to the plasma core. Again, model results do not fit experimental data outwards from $\rho = 0.546$ to $\rho = 0.703$, reinforcing that different physics dominates in the outer LHD plasma.

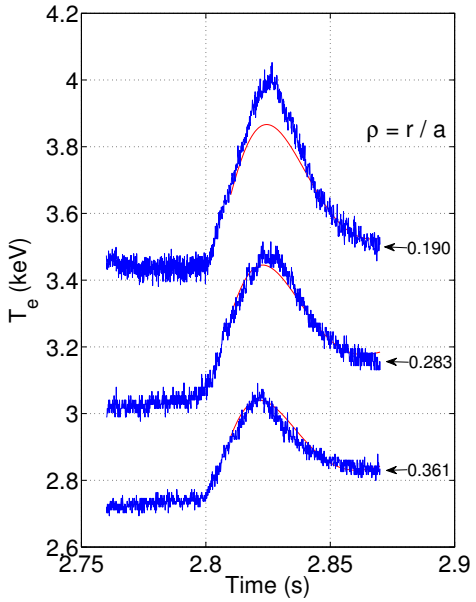

Figure 3. Time evolution of electron temperature at three specific radii selected from Fig.1 for the central temperature rise(R) case, during the heat pulse propagation experiment in LHD plasma #Te49708. Data and model output are denoted by blue and red lines respectively.

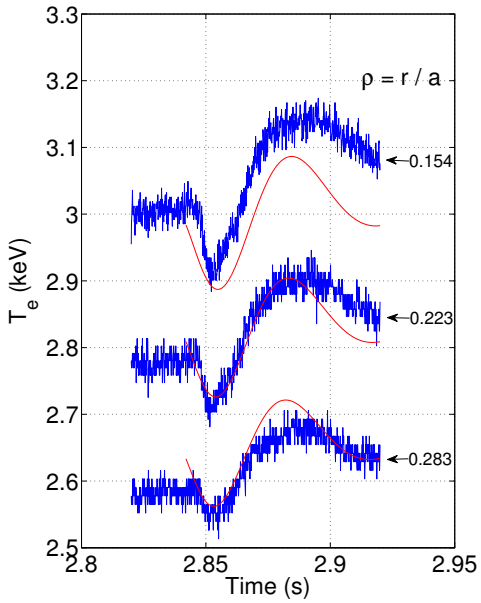

Figure 4. Time evolution of electron temperature at three specific radii selected from Fig.2 for the central temperature drop(D) case, during the heat pulse propagation experiment in LHD plasma #Te49719. Data and model output are denoted by blue and red lines respectively.

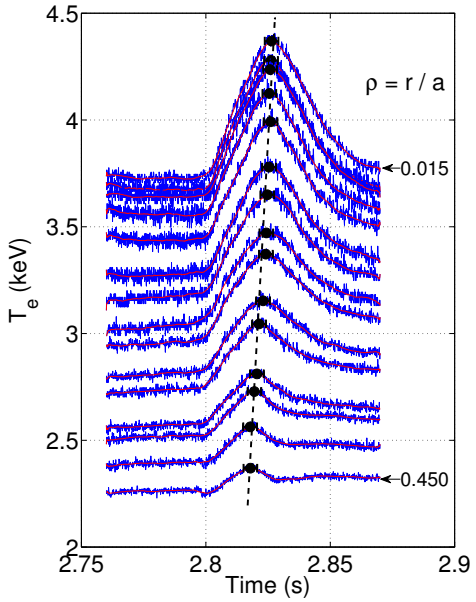

Figure 5. Data analysis underpinning calculation of pulse velocity from the experimental data, which requires a statistically robust identification of the time of the pulse peak from the noisy data at each radius $0.450 \geq \rho \geq 0.015$. Blue lines show timeseries of electron temperature data versus time from the R case(Te49708). Red lines denote timeseries smoothed over a window whose span is 5% of the total sample points, so that approximately 50 sample points generate the moving average. Black dots mark the maximum values, at each radius, of each smoothed time-evolving electron temperature pulse. The width of the horizontal error bars is defined by span of the moving window. The black dash line is the best fit straight line joining all the peaks. From it we infer the pulse propagation speed, which is nearly independent of radius, to be $(32.62 \pm 9.89)\, ms^{-1}$.

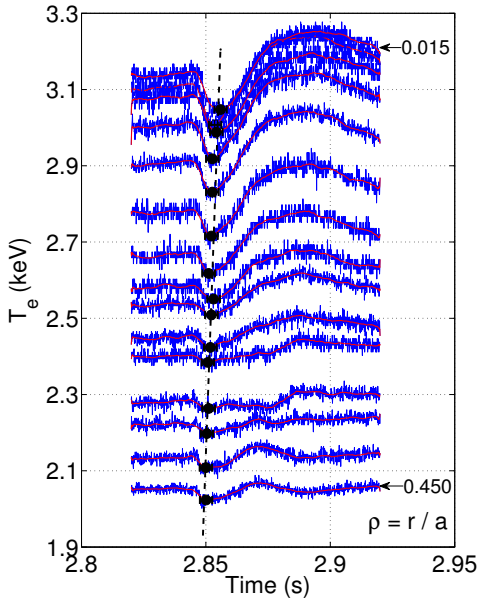

Figure 6. As Fig.5, demonstrating the calculation of the pulse velocity for the electron temperature data for the D case. Despite data which is more noisy than in Fig.5, the pulse propagation velocity calculated from the dashed line is approximately constant across all radii in this region $0.450 \geq \rho \geq 0.015$ of LHD plasma 49719. We infer a pulse velocity $(53.50 \pm 20.97)\, ms^{-1}$.

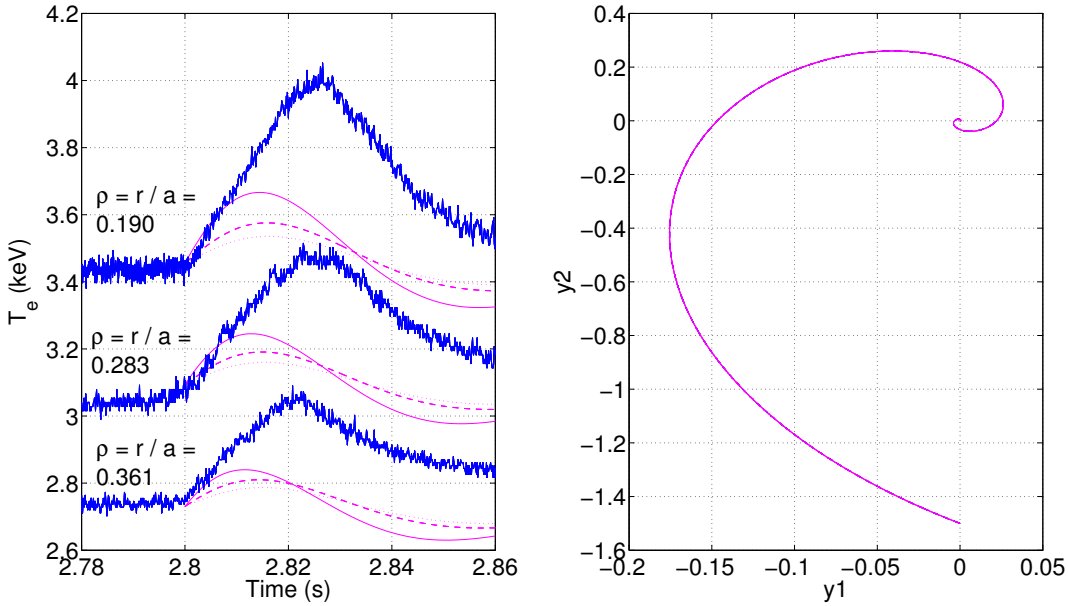

Figure 7. Variation and robustness of nonlinear pulse phenomenology in the model, for three different values of pseudo-velocity v_0 at three radial locations(Left panel). Blue lines show experimental data for R case in plasma 49708. Solid, dash and dot magenta lines denote simulation outputs for $v_0 = 15, v_0 = 30$ and $v_0 = 45$ respectively. The boundary condition for R case is $y_2(0) = 1.5$, and no horizontal or vertical shift is applied to the model outputs. (Right panel)Phase plot of model outputs from left plots, all of which lie on the same orbit. Circulation direction of this phase plot is identical with Fig.6(a) of Ref.[25], where the sign of the horizontal axis is reversed.

Acknowledgements

This work was part-funded by the RCUK Energy Programme under grant EP/I501045. This project has received funding from the European Union's Horizon 2020 research and innovation programme under grant agreement number 633053. The views and opinions expressed herein do not necessarily reflect those of the European Commission. This work was also supported in part by the grant-in-aid for scientific research of JSPF, Japan (23244113) and KAKENHI (21224014) from JSPS, Japan. This work was also supported in part by the Grant-in-Aid for Scientific Research of JSPF, Japan (23360414) and by the collaboration programs of the National Institute for Fusion Science (NIFS) (NIFS13KOCT001) and the Research Institute for Applied Mechanics of Kyushu University.

---

[1] P.H. Diamond, A. Hasegawa and K. Mima, Plasma Phys. Control. Fusion **53**, 124001 (2011).

[2] G.R. Tynan, A. Fujisawa and G. McKee, Plasma Phys. Control. Fusion **51**, 113001 (2009).

[3] P.H. Diamond, S.-I. Itoh, K. Itoh and T.S. Hahm, Plasma Phys. Control. Fusion **47**, R35 (2005).

[4] J.M. Dewhurst, B. Hnat, N. Ohno, R.O. Dendy, S. Masuzaki, T. Morisaki and A. Komori, Plasma Phys. Control. Fusion **50**, 095013 (2008).

[5] D.K. Gupta, R.J. Fonck, G.R. McKee, D.J. Schlossberg and M.W. Shafer, Phys. Rev. Lett. **97**, 125002 (2006).

[6] S. Coda, M. Porkolab and K.H. Burrell, Phys. Rev. Lett. **86**, 4835 (2001).

[7] R. Sanchez, D.E. Newman, J.-N. Leboeuf, V.K. Decyk and B.A. Carreras, Phys. Rev. Lett. **101**, 205002 (2008).

[8] C. Hidalgo, C. Silva, B.A. Carreras, B. van Milligen, H. Figueiredo, L. Garca, M.A. Pedrosa, B. Gonalves and A. Alonso, Phys. Rev. Lett. **108**, 065001 (2012).

[9] S.C. Chapman, R.O. Dendy and B. Hnat, Phys. Rev. Lett. **86**, 2814 (2001).

[10] H. Zhu, S.C. Chapman and R.O. Dendy, Phys. Plasmas **20**, 042302, (2013).

[11] H. Zhu, S.C. Chapman, R.O. Dendy and K. Itoh, Phys. Plasmas **21**, 062307, (2014).

[12] G.M.D. Hogeweij, J. O'Rourke and A.C.C. Sips, Plasma Phys. Control. Fusion **33**, 189 (1991).

[13] B.J.D. Tubbing, N.J. Lopes Cardozo and M.J. Van der Wiel, Nucl. Fusion **27**, 1843 (1987).

[14] T.C. Luce, C.C. Petty and J.C.M. de Haas, Phys. Rev. Lett. **68**, 52 (1992).

[15] J.C. DeBoo, C.C. Petty, A.E. White, K.H. Burrell, E.J. Doyle, J.C. Hillesheim, C. Holland, G.R. McKee, T.L. Rhodes, L. Schmitz, S.P. Smith, G. Wang and L. Zeng, Phys. Plasmas **19**, 082518, (2012).

[16] C.C. Petty and T.C. Luce, Nucl. Fusion **34**, 121 (1994).

[17] S. Inagaki, H. Takenaga, K. Ida, A. Isayama, N. Tamura, T. Takizuka, T. Shimozuma, Y. Kamada, S. Kubo, Y. Miura, Y. Nagayama, K. Kawahata, S. Sudo, K. Ohkubo, LHD Experimental group and the JT-60 Team, Nucl. Fusion **46**, 133 (2006).

[18] H. Sun, X. Ding, L. Yao, B. Feng, Z. Liu, X. Duan and Q. Yang, Plasma Phys. Control. Fusion **52**, 045003 (2010).

[19] J.E. Rice, C. Gao, M.L. Reinke, P.H. Diamond, N.T. Howard, H.J. Sun, I. Cziegler, A.E. Hubbard, Y.A. Podpaly, W.L. Rowan, J.L. Terry, M.A. Chilenski, L. Delgado-Aparicio, P.C. Ennever, D. Ernst, M.J. Greenwald, J.W. Hughes, Y. Ma, E.S. Marmar, M. Porkolab, A.E. White and S.M. Wolfe, Nucl. Fusion **53**, 033004 (2013).

[20] G.W. Spakman, G.M.D. Hogeweij, R.J.E. Jaspers, F.C. Schller, E. Westerhof, J.E. Boom, I.G.J. Classen, E. Delabie, C. Domier, A.J.H. Donne, M.Yu. Kantor, A. Kramer-Flecken, Y. Liang, N.C. Luhmann Jr, H.K. Park, M.J. van de Pol, O. Schmitz, J.W. Oosterbeek and the TEXTOR Team, Nucl. Fusion **48**, 115005 (2008).

[21] D.L. Brower, S.K. Kim, K.W. Wenzel, M.E. Austin, M.S. Foster, R.F. Gandy, N.C. Luhmann, Jr., S.C. McCool, M. Nagatsu, W.A. Peebles, Ch.P. Ritz and C.X. Yu, Phys. Rev. Lett. **65**, 337 (1990).

[22] P. Mantica, P. Galli, G. Gorini, G.M.D. Hogeweij, J. de Kloe, N.J. Lopes Cardozo and RTP Team, Phys. Rev. Lett. **82**, 5048 (1999).

[23] E.D. Fredrickson, J.D. Callen, K. McGuire, J.D. Bell, R.J. Colchin, P.C. Efthimion, K.W. Hill, R. Izzo, D.R. Mikkelsen, D.A. Monticello, V. Pare, G. Taylor and M. Zarnstorff, Nucl. Fusion **26**, 849 (1986).

[24] S. Inagaki, N. Tamura, K. Ida, K. Tanaka, Y. Nagayama, K. Kawahata, S. Sudo, K. Itoh, S-I. Itoh, A. Komori and LHD Experimental Group, Plasma Phys. Control. Fusion **52**, 075002 (2010).

[25] R.O. Dendy, S.C. Chapman and S. Inagaki, Plasma Phys. Control. Fusion **55**, 115009 (2013).

[26] N. Tamura, S. Inagaki, K. Tanaka, C. Michael, T. Tokuzawa, T. Shimozuma, S. Kubo1, R. Sakamoto, K. Ida, K. Itoh, D. Kalinina, S. Sudo, Y. Nagayama, K. Kawahata, A. Komori

315 and LHD Experimental Group, Nucl. Fusion **47**, 449 (2007).
316 [27] S. Inagaki, K. Ida, N. Tamura, T. Shimozuma, S. Kubo, Y. Nagayama, K. Kawahata, S. Sudo,
317 K. Ohkubo and LHD Experimental Group, Plasma Phys. Control. Fusion **46**, A71 (2004).
318 [28] S.P. Eury, E. Harauchamps, X. Zou, and G. Giruzzi, Phys. Plasmas **12**, 102511, (2005).
319 [29] N.J. Lopes Cardozo, Plasma Phys. Control. Fusion **37**, 799 (1995).
320 [30] F. Ryter, R. Dux, P. Mantica and T. Tala, Plasma Phys. Control. Fusion **52**, 124043 (2010).
321 [31] N.A. Kudryashov, Commun Nonlinear Sci Numer Simulat **14**, 1891-1900 (2009).
322 [32] X. Garbet, Y. Sarazin, F. Imbeaux, P. Ghendrih, C. Bourdelle, O.D. Gurcan and P.H. Dia-
323 mond, Phys. Plasmas **14**, 122305, (2007).